Improved Concept and Model of Eddy Current Damper

Henry A. Sodano
Assistant Professor
Mechanical Engineering Department,
Michigan Technological University,
1400 Townsend Dr.,
Houghton, MI 49931
e-mail: hsodano@mtu.edu

Jae-Sung Bae
Senior Researcher
Wind Power/Fluid Machinery Research Center,
Department of New & Renewable Energy Research,
Korea Institute of Energy Research
e-mail: jsbae@kier.re.kr

Daniel J. Inman
Professor, Director
Center for Intelligent Material Systems and Structures,
Virginia Polytechnic Institute and State University,
Blacksburg, VA 24061-0261
e-mail: dinman@vt.edu

W. Keith Belvin
Structural Dynamics Branch,
NASA Langley Research Center,
Hampton, VA 23681-0001
e-mail: w.k.belvin@larc.gov

When a conductive material experiences a time-varying magnetic field, eddy currents are generated in the conductor. These eddy currents circulate such that they generate a magnetic field of their own, however the field generated is of opposite polarity, causing a repulsive force. The time-varying magnetic field needed to produce such currents can be induced either by movement of the conductor in the field or by changing the strength or position of the source of the magnetic field. In the case of a dynamic system the conductor is moving relative to the magnetic source, thus generating eddy currents that will dissipate into heat due to the resistivity of the conductor. This process of the generation and dissipation of eddy current causes the system to function as a viscous damper. In a previous study, the concept and theoretical model was developed for one eddy current damping system that was shown to be effective in the suppression of transverse beam vibrations. The mathematical model developed to predict the amount of damping induced on the structure was shown to be accurate when the magnet was far from the beam but was less accurate for the case that the gap between the magnet and beam was small. In the present study, an improved theoretical model of the previously developed system will be formulated using the image method, thus allowing the eddy current density to be more accurately computed. In addition to the development of an improved model, an improved concept of the eddy current damper configuration is developed, modeled, and tested. The new damper configuration adds significantly more damping to the structure than the previously implemented design and has the capability to critically damp the beam's first bending mode. The eddy current damper is a noncontacting system, thus allowing it to be easily applied and able to add significant damping to the structure without changing dynamic response. Furthermore, the previous model and the improved model will be applied to the new damper design and the enhanced accuracy of this new theoretical model will be proven. [DOI: 10.1115/1.2172256]

Keywords: eddy current damper, magnetic damping, passive vibration suppression, viscous damping

1 Introduction

When a nonmagnetic conductive metal is placed in a magnetic field, eddy currents are generated. These eddy currents circulate in such a way that they induce their own magnetic field with opposite polarity of the applied field, causing a resistive force. However, due to the electrical resistance of the metal, the induced currents will dissipated into heat at the rate of I^2R and the force will disappear. In the case of a dynamic system the conductive metal is continuously moving in the magnetic field and experiences a continuous change in flux that induces an electromotive force (emf), allowing the induced currents to regenerate. The process of the eddy currents being generated causes a repulsive force to be produced that is proportional to the velocity of the conductive metal. Since the currents are dissipated, energy is being removed from the system, thus allowing the magnet and conductor to function like a viscous damper. The use of eddy currents for damping of dynamic systems has been known for decades and its application to magnetic braking systems [1–4] and lateral vibration control of rotating machinery [5,6] has been thoroughly investigated.

While the theory and applications of rotary magnetic braking systems have been well documented, there are many more applications of eddy current dampers. Karnopp [7] introduced the idea that a linear electrodynamic motor consisting of coils of copper wire and permanent magnets could be used as an electromechanical damper for vehicle suspension systems. He showed that his actuator could be much smaller and lighter than conventional actuators while still providing effective damping in the frequency range typically encountered by road vehicle suspension systems. Schmid and Varga [8] studied a vibration-reducing system with eddy current dampers (ECDs) for high resolution and nanotechnology devices such as an STM (scanning tunneling microscope). Teshima et al. [9] investigated the effects of an eddy current damper on the vibrational characteristics of superconducting levitation and showed that the damping of vertical vibrations was about 100 times improved by eddy current dampers. Lee [10] considered the dynamic stability of conducting beam plates in transverse magnetic fields. The research showed that three regions of stability existed: damped stable oscillation, static asymptotic stability, and static divergence instability. The buckling field was also found to exhibit a linear dependence on the geometry of the ratio of the thickness and length of the beam plate.

Kobayashi and Aida [11] explored the use of a Houde damper (a type of damped vibration absorber) using an eddy current damper as the energy dissipation mechanism. The eddy current damper consisted of a conducting plated moving between two permanent magnets. The study found the Houde damper could increase the damping ratio by 2% and suppress the displacement of the pipe by a factor of 8 to 10. Kienholtz et al. [12] investigated the use of a magnetic tuned mass damper for vibration suppression of a spacecraft solar array and a magnetically damped isolation mount for the payload inside of a space shuttle. The magnetic tuned mass damper system targeted two modes of the solar array (first torsion at 0.153 Hz and first out of plane bending of 0.222 Hz) and increased the damping by 30 and 28 dB, respec-

Contributed by the Technical Committee on Vibration and Sound of ASME for publication in the JOURNAL OF VIBRATION AND ACOUSTICS. Manuscript received August 24, 2004; final manuscript received November 3, 2005. Assoc. Editor: Shirley J. Dyke.

 Copyright © 2006 by ASME

tively, while the higher frequency untargeted modes 0.4–0.8 Hz were damped in the range of 11–16 dB. Hahn et al. [13] studied the damping characteristics of a permanent magnet moving inside of a conducting tube. Their work performs an experimental and theoretical analysis of the systems and determines the amount of damping that can be expected for any pipe configuration. Graves et al. [14] derived the mathematical model of electromagnetic dampers based on motional emf and transformer emf devices and presented a theoretical comparison between these two devices. A motional emf device generates eddy currents due to the movement of a closed conduction circuit or a conductor through a stationary magnetic field, while a transformer emf device generates an emf within a stationary conducting circuit, due to a time-varying magnetic field. Both of these electromagnetic devices can be used for vibration damping purposes.

While the aforementioned studies have investigated a variety of applications, several studies have been performed to determine the effect of magnetic fields on the vibration of beams. Morisue [15] investigated the effect of an applied magnetic field on a conducting cantilever beam and analyzed the beam response. The response was predicted using finite difference methods and the results were found to compare well with experiments performed at Argonne National Laboratory. In a similar study Takagi et al. [16] studied the deflection of a thin copper plate subjected to magnetic fields both analytically and experimentally. They used an electromagnet with very high current (several hundred amperes) to generate the magnetic field, then analyzed the response of the plate to the applied field. Matsuzaki et al. [17] proposed the concept of a new vibration control system in which the vibration of a beam periodically magnetized along the span is suppressed using electromagnetic forces generated by a current passing between the magnetized sections. To confirm the vibration suppression capabilities of their proposed system, they performed a theoretical analysis of a thin beam with two magnetized segments subjected to an impulsive force and showed the concept to be viable. Following the proposal of the previous concept, Matsuzaki et al. [18] performed an experimental study to show the effectiveness of this new concept. However, a partially magnetized beam was not available to the authors, so a thin beam with a current carrying wire bonded to its surface along with a permanent magnet was used. The system was then used to determine if the electromagnetic force generated by the wire was sufficient to suppress the vibration of the beam. The results of their study showed that indeed the force is capable of damping the beam's first few modes of vibration.

Recently, Kwak et al. [19] investigated the effects of an eddy current damper on the vibration of a cantilever beam and their experimental results showed that the eddy current damper can be an effective device for vibration suppression. The authors ECD used a fixed copper conducting plate and flexible linkage attached to the tip of the beam in order to utilize the axial magnetic flux and generate eddy current damping forces. Bae et al. [20] modified and developed the theoretical model of the eddy current damper constructed by Kwak et al. [19]. Using this new model, the authors investigated the damping characteristics of the ECD and simulated the vibration suppression capabilities of a cantilever beam with an attached ECD numerically.

When using eddy currents, the typical method of inducing an emf in the conductive metal is to place the metal directly between two oppositely poled magnets with the metal moving perpendicular to the magnets poling axis; a schematic of this process is shown in Fig. 1 and has been studied in Refs. [1–8,11,12,14,19,20]. This configuration is optimal because of the concentrated magnetic field between the two magnets. While this configuration is effective for magnetic braking, in certain applications it is not possible. The research presented by Sodano et al. [21] proposed and developed a theoretical model of one such system in which the transverse vibrations of a cantilever beam were damped by a permanent magnet fixed to a location perpendicular

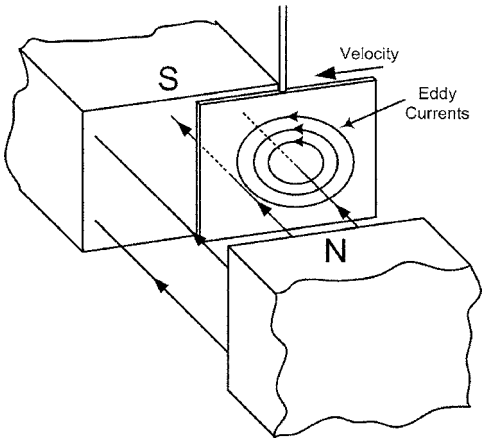

Fig. 1 Schematic of conductive material passing through a magnetic field and the generation of eddy currents

to the beams motion and the magnet's radial flux was used to generate the damping force. It was shown through experiments that the theoretical model very accurately estimated the damping when the magnet was greater than 5 mm from the beam, but was less accurate for smaller gaps. The present study will revisit the theoretical model of the system developed by Sodano et al. [21] and provide improvements to its accuracy over the whole range of magnet locations. Additionally, this manuscript will present an enhanced concept for the eddy current damper. Like the damper used in the study by Sodano et al. [21] the proposed damper uses the radial magnetic flux of the permanent magnet to suppress the vibrations of the beam. However, in the previous study only one magnet was used. In the present study, it is realized that when two similar magnetic poles are placed close to each other, the magnetic flux of each magnet is compressed in the poling direction, causing the intensity in the radial direction to be enhanced as shown in Fig. 2. The increased flux in the radial direction causes the magnetic damper to be far more effective than the use of a single magnet. Furthermore, since the ECD of Refs. [19,20] was installed at the tip of the beam, the dynamic characteristics of the beam were changed considerably. However, the eddy current damper developed by Sodano et al. [21] and the concept detailed in this manuscript do not contact the structure, thus allowing them to add significant damping to the system without changing the dynamics of the structure.

In this manuscript the magnetic flux generated by a cylindrical permanent magnet will be calculated, allowing the eddy current density to be determined. After finding the eddy current density, the image method described by Lee and Park [22] will be used to enforce the necessary boundary condition of zero eddy current density at the edges of the conductor. By doing this, the accuracy of the predicted damping force will be improved over the tested range of distances between the magnet and beam. The modifications of the model will be applied to the eddy current damper previously developed by Sodano et al. [21] and the increased ac-

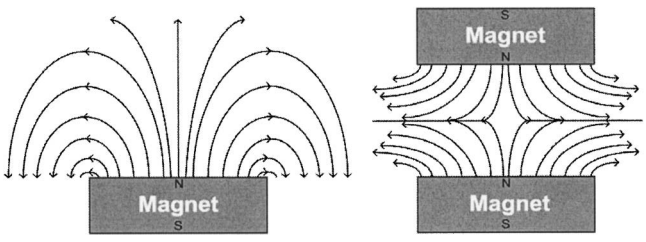

Fig. 2 Schematic showing the magnetic flux of one and two magnets

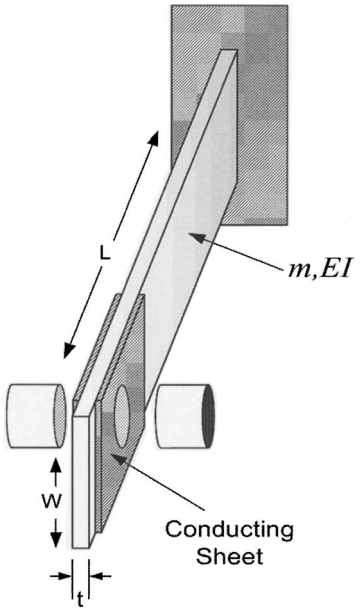

Fig. 3 Cantilever beam in magnetic field generated by permanent magnet

curacy due to these improvements will be shown through a comparison of both models with experimental data. Lastly, a new eddy current damper concept will be detailed. The improved model will be applied to this new damper and the model's accuracy will be validated through experimental results. It will be shown that the new damping concept provides significantly more damping to the structure than the previously developed damper.

2 Eddy Current Damping Model

2.1 Model of Induced Eddy Currents. Figure 3 depicts the configuration of our eddy current damping system, which consists of a cantilever beam with a copper conducting plate located in the magnetic field generated by a single cylindrical permanent magnet. Due to the permanent magnet, a magnetic field is generated in the vertical (z) and horizontal or radial (y or R) axes. The configuration of the damper is shown in Fig. 4 and consists of a conducting sheet of thickness δ and conductivity σ moving with velocity $\mathbf{v}$ in the air gap l_g of a circular magnet. When the beam surface is deflected and set in motion in the static magnetic field, an electric field is generated in the conducting sheet. Since the deflection of the beam is in the vertical direction, the vertical component of the magnetic field does not contribute to the generation of eddy currents. Hence, the electric field on the conductor is dependent on the horizontal component B_y of the magnetic field. As shown in Fig. 4, the eddy currents circulate on the conducting sheet in the x-y plane, causing a magnetic field to be generated.

If the surface charges are assumed to be ignored, the current density $\mathbf{J}$ induced in the conducting sheet moving in the vertical direction is given by

$$\mathbf{J} = \sigma(\mathbf{v} \times \mathbf{B}) \tag{1}$$

where the $\mathbf{v} \times \mathbf{B}$ term is an electromotive force driving the eddy currents $\mathbf{J}$. The velocity and magnetic flux can be written as follows

$$\mathbf{v} = 0\mathbf{i} + 0\mathbf{j} + v_z\mathbf{k} \tag{2}$$

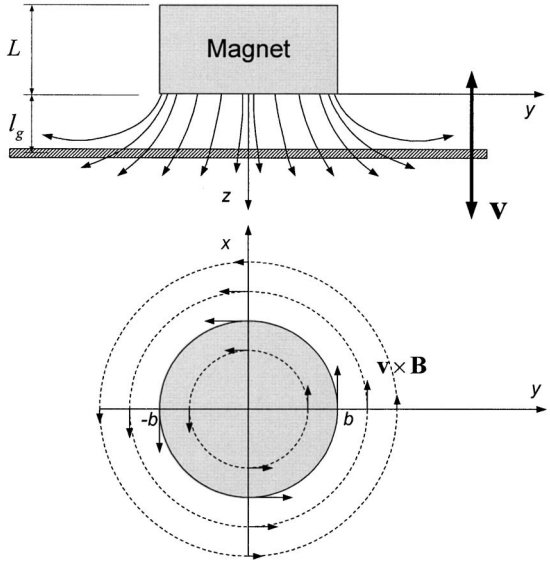

Fig. 4 Magnetic field and the eddy currents induced in the cantilever beam

$$\mathbf{B} = B_x\mathbf{i} + B_y\mathbf{j} + B_z\mathbf{k} \tag{3}$$

where the velocity is only in the z direction. Substitution of Eqs. (2) and (3) into Eq. (1) allows the eddy current density to be defined by

$$\mathbf{J} = \sigma(\mathbf{v} \times \mathbf{B}) = \sigma v_z(-B_y\mathbf{i} + B_x\mathbf{j}) \tag{4}$$

The above equation shows that the magnetic flux in the z direction has no effect on the induced eddy currents and that the induced currents are solely dependent on the x and y components of the magnetic flux or the flux tangential to the face of the conducting sheet.

The magnetic flux density due to a circular magnetized strip, shown in Fig. 5, can be written by [23]

$$d\mathbf{B} = \frac{\mu_0 M_0}{4\pi}\int_0^{2\pi}\frac{d\mathbf{l} \times \mathbf{R}_1}{R_1^3}d\phi \tag{5}$$

where μ_0 and M_0 are the permeability and the magnetization per unit length, respectively. The vector $\mathbf{R}_1$ is defined by the distance between the differential element on the circular strip and the point on the y-z plane as shown in Fig. 4 and defined as

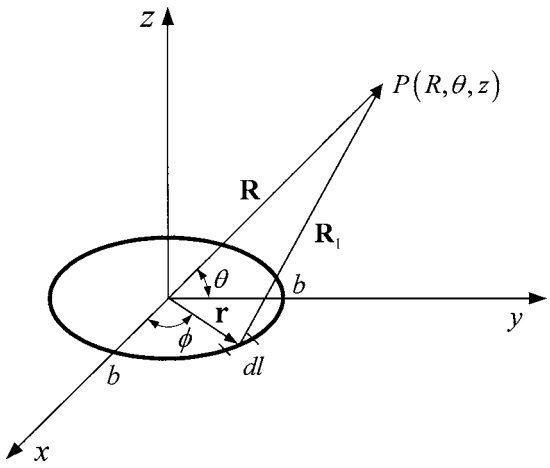

Fig. 5 Schematic of the circular magnetized strip depicting the variable used in the analysis

$$\mathbf{R}_1 = \mathbf{R} - \mathbf{r} \tag{6}$$

where

$$\mathbf{R} = y\mathbf{j} + z\mathbf{k} \tag{7}$$

$$\mathbf{r} = b\cos\phi\mathbf{i} + b\sin\phi\mathbf{j} \tag{8}$$

The length vector $d\mathbf{l}$ of the infinitesimal strip is

$$d\mathbf{l} = -b\sin\phi d\phi\mathbf{i} + b\cos\phi d\phi\mathbf{j} \tag{9}$$

where b is the radius of the circular magnet.

Substituting Eqs. (6) and (9) into Eq. (5), the magnetic flux density due to the circular magnetized strip is

$$dB_y = \frac{\mu_0 z M_0 b}{4\pi}\int_0^{2\pi}\frac{\sin\phi}{(b^2+y^2+z^2-2yb\sin\phi)^{3/2}}d\phi$$

$$= \frac{\mu_0 z M_0 b}{4\pi} I_1(b,y,z) \tag{10}$$

$$dB_z = \frac{\mu_0 M_0 b}{4\pi}\int_0^{2\pi}\frac{b-y\sin\phi}{(b^2+y^2+z^2-2yb\sin\phi)^{3/2}}d\phi$$

$$= \frac{\mu_0 M_0 b}{4\pi} I_2(b,y,z) \tag{11}$$

where I_1 and I_2 include the elliptic integrals and are shown in the Appendix. Hence, the magnetic flux density due to the circular magnet of length L is written by

$$B_y(y,z) = \frac{\mu_0 M_0 b}{4\pi}\int_{-L}^{0}(z-z')I_1(b,y,z-z')dz' \tag{12}$$

$$B_z(y,z) = \frac{\mu_0 M_0 b}{4\pi}\int_{-L}^{0} I_2(b,y,z-z')dz' \tag{13}$$

where z' and L are the distance in the z direction from the center of a magnetized infinitesimal strip and the length of the circular magnet, respectively. As indicated in Fig. 2, the magnetic field distributions in Eqs. (12) and (13) are symmetric about the z axis.

Since the velocity of the conducting sheet is in the z direction, the magnetic flux density B_z does not contribute to the damping force. Using Eqs. (1), (12), and (13), the damping force due to the eddy current is defined by

$$\mathbf{F} = \int_V \mathbf{J}\times\mathbf{B}dV = -\mathbf{k}\sigma\delta v\int_0^{2\pi}\int_0^{r_c} yB_y^2(y,l_g)dyd\phi$$

$$= -\mathbf{k}2\pi\sigma\delta v\int_0^{r_c} yB_y^2(y,l_g)dy \tag{14}$$

where δ and v are the thickness and the vertical velocity of the conducting sheet, respectively, r_c is the equivalent radius of the conductor that preserves its surface area, and l_g is the distance between the conducting sheet and the bottom of the magnet as shown in Fig. 4.

2.2 Application of the Image Method to Improve Model Accuracy. The derivation performed in Sec. 2.1 is valid for the case of an infinite conducting sheet, meaning that the edge effects of the conductor are unaccounted for. Neglecting the edge effects in the model will cause the predicted damping to be greater than actually present, because the eddy current density is not required to be zero at the edges. In order to account for the edge effects, the image method [22] can be used to satisfy the boundary condition of zero eddy current density at the conducting plate's boundaries. A schematic showing how the image method is used can be seen in Fig. 6. By introducing an imaginary eddy current density the net eddy current in the radial direction $\mathbf{J}'$ can be written as

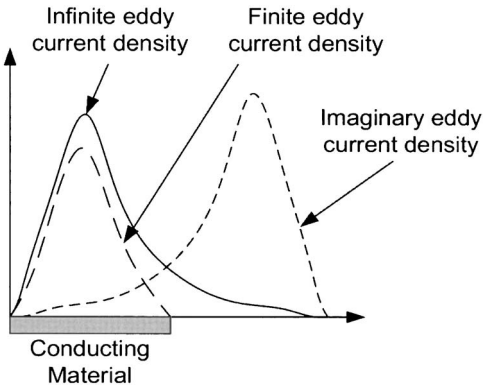

Fig. 6 Schematic demonstrating the effect of the imaginary eddy currents

$$\mathbf{J}' = (J_y^{(1)} - J_y^{(2)}) \tag{15}$$

where y is the radial direction and the imaginary eddy current density is written as

$$J_y^{(2)}(y) = J_y^{(1)}(2A-y) \tag{16}$$

where $J_y^{(1)}$ is the predicted eddy current density and the dimension A corresponds to half the length of the conducting plate as shown in Fig. 7. Only one imaginary eddy current is needed because the conductor is modeled as a circular plate with the same area as the original conductor as shown in Fig. 7. This assumption is made to simplify the integration of Eqs. (12)–(14). Substituting Eqs. (15) and (16) into Eq. (14), the damping force accounting for the imaginary eddy currents is defined as

$$\mathbf{F} = \int_V \mathbf{J}'\times\mathbf{B}dV = -\mathbf{k}\sigma\delta v\left(\int_0^{2\pi}\int_0^{r_c} yB_y^2(y,l_g)dyd\phi - \int_0^{2\pi}\int_0^{r_c} yB_y^2(2A-y,l_g)dyd\phi\right)$$

$$= -\mathbf{k}2\pi\sigma\delta v\left(\int_0^{r_c} yB_y^2(y,l_g)dy - \int_0^{r_c} yB_y^2(2A-y,l_g)dy\right) \tag{17}$$

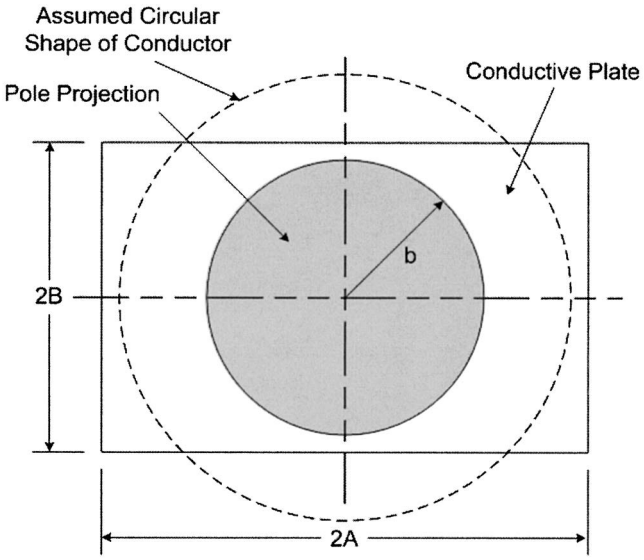

Fig. 7 Schematic showing the variables associated with the conducting plate

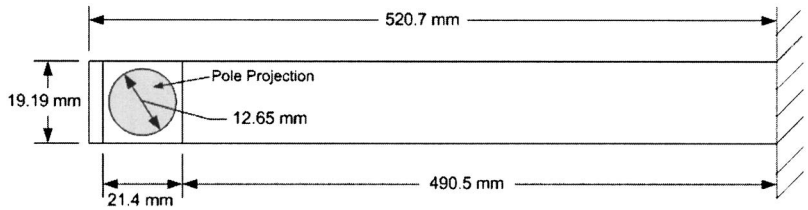

Fig. 8 Schematic showing the dimensions of the beam

Because it is too difficult to integrate Eqs. (12) and (13) analytically, a numerical integration method is used to obtain the damping force in Eq. (17).

2.3 Modeling of Cantilever Beam. The dynamic model of the cantilever beam is formulated using energy methods. The derivation of this system starts by defining the kinetic energy, potential energy, and external work as:

$$T = \frac{1}{2}\int_V \rho \dot{u}(x,t)^T \dot{u}(x,t) dV \tag{18}$$

$$U = \frac{1}{2}\int_V \underline{S}^T E \underline{S} dV \tag{19}$$

$$F\delta x = Q_e \delta u_e + F\delta u(x,t) \tag{20}$$

where $u(x,t)$ is the displacement of the beam, ρ is the density, V is the volume of the beam, F is a concentrated force acting on the beam, E is the modulus of elasticity, and S is the strain of the beam. The term Q_e describes the nonconservative forces due to the induced eddy currents and is written as:

$$Q_e = -c_e \dot{u}(x_e,t) = -c_e \dot{u}_e \tag{21}$$

where c_e is the viscous damping force from the eddy currents. By Hamilton's principle, the variation of the energy in the system must balance to zero as follows:

$$\int_{t_1}^{t_2} (\delta U + \delta T - F\delta x) dt = 0 \tag{22}$$

Taking the variation of the kinetic and potential energy from Eq. (22) yields:

$$\delta U = \int_V \delta \underline{S}^T E \underline{S} dV \tag{23}$$

$$\delta T = \int_V \rho \delta \dot{u}^T \dot{u} dV \tag{24}$$

The variations found in Eqs. (20), (23), and (24) can be substituted into Eq. (22) to obtain the variational equation below:

$$\int_{t_1}^{t_2} \left(\int_V \rho \delta \dot{u}^T \dot{u} dV - \int_V \delta \underline{S}^T E \underline{S} dV + \delta u(x_i) \cdot F(x_i) - \delta \dot{u}(x_i) \cdot Q_e(x_i) \right) = 0 \tag{25}$$

Before solving Eq. (25) for the cantilever beam some assumptions are made. The first assumption follows the assumed modes procedure, which says that the displacement of the beam can be written as the summation of modes in the beam and a temporal coordinate [18]:

$$u(x,t) = \sum_{i=1}^{N} \phi_i(x) r_i(t) = \underline{\phi}(x) \underline{r}(t) \tag{26}$$

where $\phi_i(x)$ is the assumed mode shapes of the structure that can be set to satisfy any combination of boundary conditions, $r(t)$ is the temporal coordinate of the displacement, and N is the number of modes to be included in the analysis. The second assumption made is to apply the Euler-Bernoulli beam theory. This allows the strain in the beam to be written as the product of the distance from the neutral axis and the second derivative of displacement with respect to the position along the beam. Once the strain is defined in this way, Eq. (26) can be used to define the strain as follows:

$$\underline{S} = -y \frac{\partial^2 u(u,t)}{\partial x^2} = -y \underline{\phi}(x)'' \underline{r}(t) \tag{27}$$

where y is the distance from the neutral axis of the beam. Using the previous two assumptions Eq. (25) can be simplified to contain terms that represent physical parameters. By doing this the equations representing the beam become more recognizable when compared to those of a typical system and help give physical meaning to the parameters in the equation of motion. The mass matrix of the system can be written as:

$$M = \int_V \rho \underline{\phi}^T(x) \underline{\phi}(x) dV \tag{28}$$

The stiffness matrix can be written as:

$$K = \int_V y^2 \underline{\phi}^T(x)'' E \underline{\phi}(x)'' dV \tag{29}$$

The parameters defined in Eqs. (28) and (29) can be substituted into Eq. (25). This substitution allows the variation to be written as:

$$\int_{t_1}^{t_2} [\delta \underline{\dot{r}}^T(t) M \underline{\dot{r}}(t) - \delta \underline{r}^T(t) K \underline{r}(t) + \delta \underline{r}(t) \varphi(x_i)^T F_i(t) - \delta \dot{u} Q_e(t)] dt = 0 \tag{30}$$

where $\delta(\,)$ indicates the variation of the corresponding variable. Taking the integral of Eq. (30) leaves the equation of motion. The following equation defines the motion of the beam:

$$M \underline{\ddot{r}}(t) + C \underline{\dot{r}}(t) + K \underline{r}(t) = \underline{\phi}(x_i)^T f_i(t) \tag{31}$$

where the damping matrix C is defined as:

$$C = [C_b + \phi_e^T c_e \phi_e] \tag{32}$$

where $\phi_e = \phi(x_e)$ with x_e defining the location of the eddy current damping force and c_e is found from the damping force of Eqs. (11). These equations now describe the dynamics of the beam and its interaction with the eddy current damper.

3 Experimental Setup

Experiments were performed on a cantilever aluminum beam in order to determine the accuracy of the model developed in this

Table 1 Physical properties of the beam, conductor and magnet

Property	Value
Young's modulus of beam	75 GPa
Density of beam	2700 kg/m^3
Conductivity of aluminum beam	3.82 x 10^7
Thickness of copper conductor	0.62 mm
Conductivity of copper conductor	5.80 x 10^7
Permanent magnet composition	NdFeB 35
Residual magnetic flux of magnet	1.21 kGauss

paper. The dimensions of the beam are shown in Fig. 8. For the experiments a neodymium-iron-boron (NdFeB) permanent magnet with radius and length of 6.35 and 12.65 mm, respectively, was used. Other relevant properties of the beam and magnet are shown in Table 1. The analysis of our system required that the eddy currents generated in the beam be included due to the high conductivity of aluminum.

The experiments performed in this study were aimed at calculating the damping ratio of the beams response for various gaps between the magnet and beam. The experimental results obtained by Sodano et al. [21] were used to simply show the improvements in the model's accuracy by incorporating the concept of the image method. However, an experimental setup similar to that of Ref. [21] was used, but the experiments performed in this study investigated the performance of an improved concept of the eddy current damper. The improved concept utilizes two permanent magnets positioned on opposite sides of the beam rather than a single magnet. The two magnets were configured such that the same magnetic poles were facing each other, causing a repulsive force between the magnets and causing the magnetic flux to be compressed along the poling axis of the magnet. The compression to the magnetic flux in this way causes its magnitude in the radial direction to be substantially increased and thus the damping force is increased. The layout of the magnets is shown in Fig. 9.

To measure the damping ratio of the beam as the distance between the magnet and the beam is varied, the frequency response was measured. The beam was excited using a piezoelectric patch mounted at the root of the beam and the displacement response at the tip of the beam was recorded using a Polytec Laser vibrometer. Once the frequency response of the system was determined, the unified matrix polynomial approach (UMPA) [24] was applied to the frequency response, allowing the damping ratio of the system to be extracted.

Additionally experiments were performed to measure the time response of the system with various gap distances. The time response of the system to an initial displacement was measured as another means of identifying the amount of damping in the system and to demonstrate the increased settling time due to the eddy currents. The initial displacement condition was applied through an electromagnet that when turned on would attract the beam, and when turned off would allow it to be released and vibrate freely. Because aluminum is not ferromagnetic, a 0.05 mm steel plate was attached to the side of the beam, allowing the beam and electromagnet to interact. This system allowed a constant initial displacement to be repeatedly applied over numerous tests and can be seen in Fig. 9.

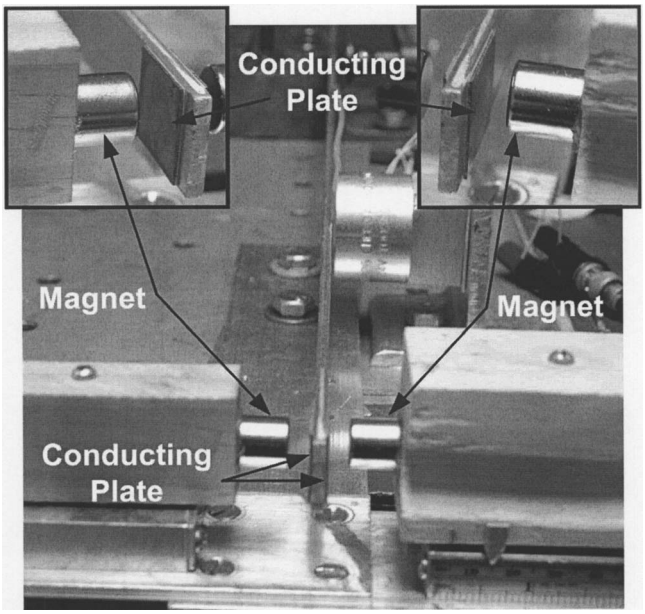

Fig. 9 Experimental setup showing position of magnets and conducting plates

4 Results and Discussion

4.1 Numerical Calculation of Magnetic Flux. To determine the damping force induced on the beam, the magnetic flux **B** must first be calculated. However, the integration of Eqs. (8) and (9) that describe the magnetic flux is too difficult to solve analytically, therefore a numerical method was used to obtain the solution. The resulting magnetic flux for the improved eddy current damper that utilizes two magnets is shown in Fig. 10. This figure shows the magnetic flux lines with the contours that represent the magnitude of the magnetic flux in the radial direction B_y. Figure 11 shows the magnet flux density in the radial direction B_y for the eddy current damper developed by Sodano et al. [21] and for the case of two magnets that is considered in this manuscript. This figure clearly shows the increase in magnetic flux thought the use of a second magnet.

After determining the magnetic flux generated by the permanent magnet, the induced eddy currents could be calculated and the damping force found. The eddy current density when the magnet is located at a distance of 1 mm from the beam is shown in Fig. 12. This figure also shows the imaginary eddy current density which was calculated using the image method and the resulting eddy current density after the image method is applied to satisfy the electrical boundary conditions of the conductor. The use of the image method allowed our theoretical model's accuracy to be greatly increased.

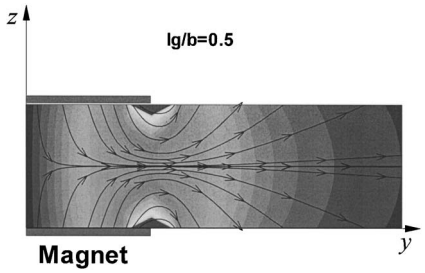

Fig. 10 Magnetic flux lines with contours of the radial flux B_y for two magnets

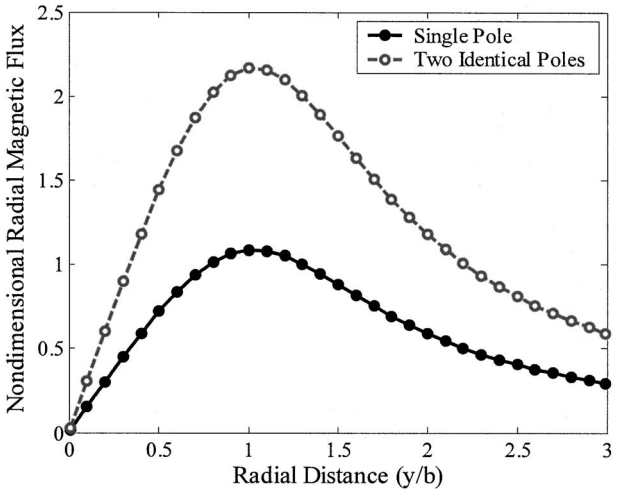

Fig. 11 Magnetic flux density B_y for a case of $l_g/b=0.2$

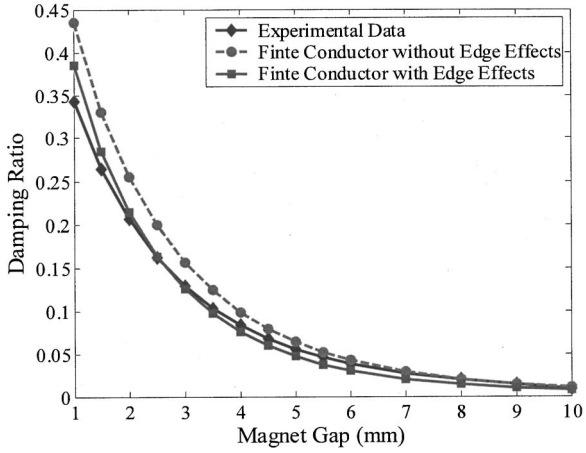

Fig. 13 Experimental and predicted damping ratio of the beam's first mode for the system used in Sodano et al. [21] and the damping ratio predicted by the improved model developed in this paper

4.2 Validation of Model Through Experiments. Once the magnetic flux and eddy current density had been numerically calculated, the accuracy of the theoretical model could be validated using the experimental setup previously detailed. The predicted and measured damping ratio of the beam was used to demonstrate the model's accuracy. As mentioned, the theoretical model developed in this study provides increased accuracy over the model previously developed by Sodano et al. [21]. To demonstrate the improvement in accuracy that is obtained through the use of the image method, Fig. 13 shows the experimental and predicted damping ratios for the eddy current damping system investigated by Sodano et al. [21] as well as the predicted damping ratio when the image method is used. From the figure, it can be seen the improved mathematical model developed in this manuscript provides a significant increase in accuracy when the magnet is in close proximity to the conductor.

Now that the improvements in the model have been confirmed, the performance of the enhanced eddy current damper can be demonstrated. In order to obtain the damping ratio from the experimental data, the UMPA method was applied to the frequency response. However, when performing the experiments it was found that the damping ratio of the first mode was overdamped for the case that the magnets were in close proximity to the beam. Therefore, in this gap range the time response of the beam when subjected to an initial displacement was measured, thus allowing the log decrement to be calculated. One experimentally obtained frequency response of the system before and after placement of the two permanent magnets is shown in Fig. 14. From this figure it is apparent that the damping of the structure is significantly increased after addition of the magnets into the system. Additionally, the use of two magnets provides significantly more vibration reduction than when one magnet is used, as done in Sodano et al. [21]. When two magnets are used the first mode is critically damped and the magnitude is suppressed by approximately 54 dB, the reductions in the magnitude of the second, third, and fourth modes are 31, 22.5, and 14 dB, respectively, whereas when one magnet was used [21], the reductions in magnitude of the first, second, and third modes were 42.4, 21.9, and 14.3 dB, respectively. Furthermore, since this eddy current damper does not contact the structure, significant damping can be added without significantly changing the dynamic response of the system, as can be seen in Fig. 14. If other passive damping methods such as constrained layer damping were to be used, the response of the structure would be considerably altered. The increased damping through the use of two magnets can also be seen in Fig. 15, which shows the time response of the beam subjected to an initial displacement when one and two magnets are located a distance of 2.5 mm. These results indicate the advantage of using the new damper configuration developed in this manuscript for the sup-

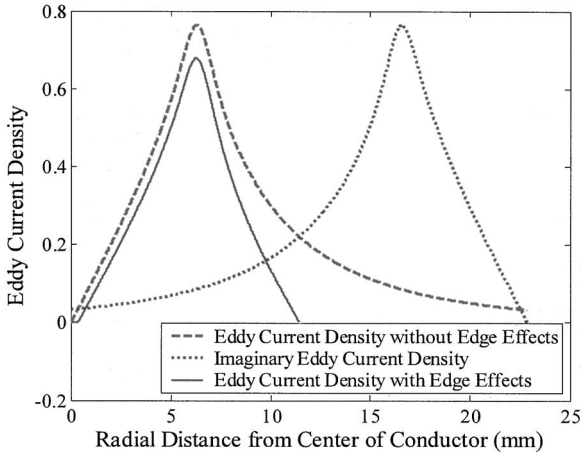

Fig. 12 Eddy current density before and after the image method is applied

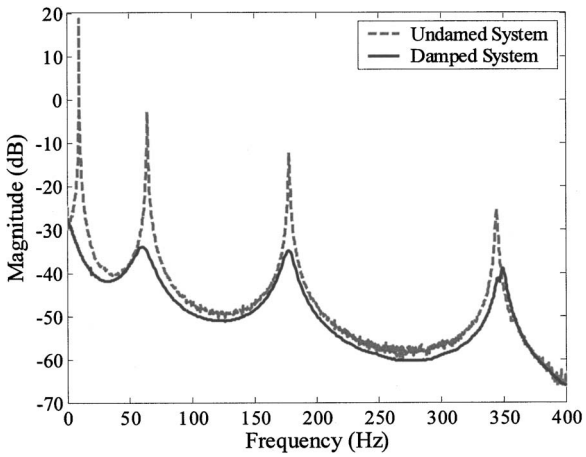

Fig. 14 Experimentally obtained frequency response of the system before and after placement of the magnets

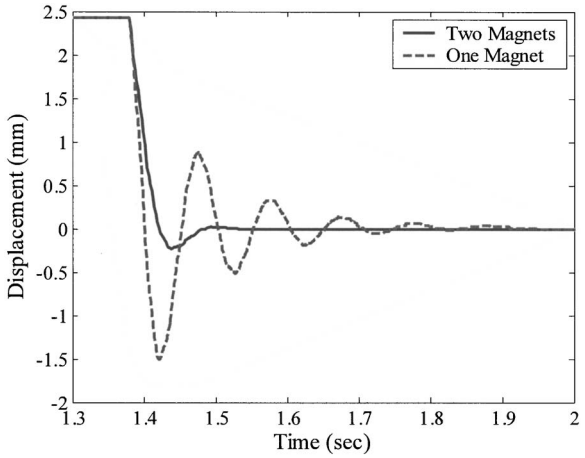

Fig. 15 Time response of the beam to an initial displacement when one and two magnets are present

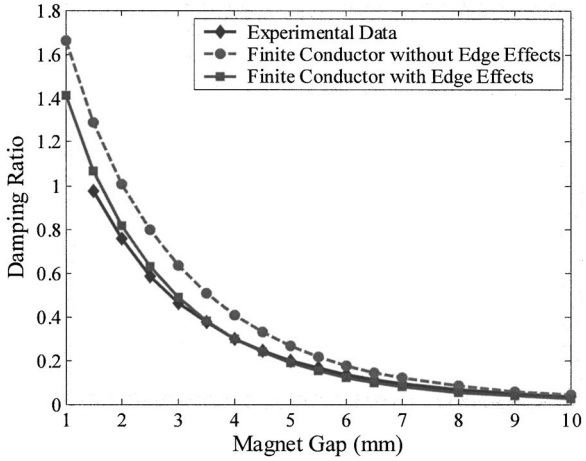

Fig. 17 Experimental and predicted damping ratio of the beam's first mode as a function of the gap between the magnet and beam

pression of transverse beam vibrations.

Using the model of the magnetic damping system, the frequency response of the beam was predicted and its accuracy was compared to the experimentally measured frequency response. A typical predicted and measured frequency response of the beam is shown in Fig. 16. To better show the accuracy of the model as the distance between the magnet and the beam is varied, the damping ratio was experimentally measured and predicted at several locations. Figure 17 shows the results of the experimental tests, the improved eddy current model that utilizes the image method, and the results using the model described by Sodano et al. [21]. It can be seen in the figure that the model of the eddy current damping system very accurately predicts the damping of the beam. Furthermore, this illustrates the improved accuracy gained through the use of the image method.

5 Conclusions

This study has developed a passive damping system that utilized the eddy currents induced in a moving conductor to suppress the vibrations of a beam. Because the damper is of passive nature it is robust to parameter changes, requires no additional energy, and is easy to apply to the structure. Furthermore, the damper developed in this paper is a noncontact damper, thus allowing significant damping to be added while allowing the other properties and dynamics of the structure to be unaffected by its addition to the system. This point is of significant importance to the many structures that were designed with specific key parameters in place, through which the addition of a damping scheme such as constrained layer damping would change. The eddy current damper developed in this paper utilized two magnets and was shown to significantly outperform previously designed systems that utilize only one magnet. A mathematical model of both the eddy current damping system and its interaction with the beam has been developed. This model of the system has been improved from earlier models through the use of the image method which allows the electrical boundary conditions of the conductor to be satisfied. The improved theoretical model has been shown to accurately predict both the frequency response and time response to an initial displacement. Furthermore, the model was used to calculate the damping ratio as the distance between the magnet and the conductor increase and compared to experimentally measured damping ratios and those predicted using a previously developed eddy current damper model. The results showed the model to be very accurate and to significantly outperform the previous model. The eddy current damper developed in this paper had the capability to provide critical damping to the first mode of vibration and reduce the second through fourth modes by 31, 22.5, and 14 dB, respectively.

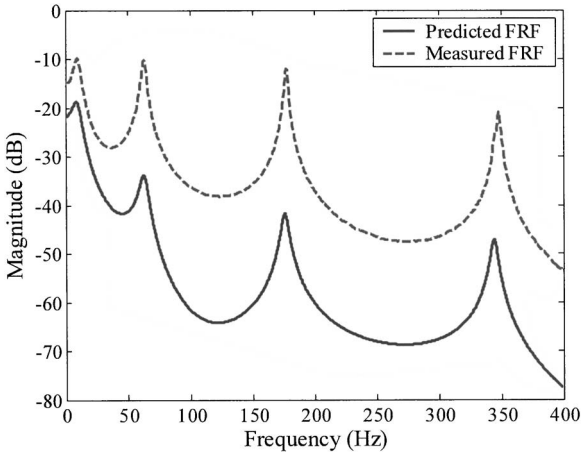

Fig. 16 Measured and predicted frequency response of the beam for the case that the magnet is located 4 mm from the beam

Acknowledgment

The authors of this paper gratefully acknowledge support from NASA's Graduate Student Researchers Program (GSRP) under Grant No. NGT-1-03020 from NASA Langley Research Center and the George R. Goodson Professorship.

Appendix

The integration I_1 in Eq. (10) is

$$I_1 = \int_0^{2\pi} \frac{\sin\phi}{(b^2+z^2-2yb\sin\phi)^{3/2}} d\phi = \frac{1}{bynp^2}\left\{ m^2\left[E_1\left(\frac{\pi}{4}, \frac{-4yb}{n^2}\right) + E_1\left(\frac{3\pi}{4}, \frac{-4yb}{n^2}\right)\right] - p^2\left[E_2\left(\frac{\pi}{4}, \frac{-4yb}{n^2}\right) + E_2\left(\frac{3\pi}{4}, \frac{-4yb}{n^2}\right)\right]\right\} \tag{A1}$$

where

$$m^2 = b^2 + y^2 + z^2 \tag{A2}$$

$$n^2 = (b-y)^2 + z^2 \tag{A3}$$

$$p = (b+y)^2 + z^2 \tag{A4}$$

The elliptic integrals of Eq. (A1) are

$$E_1 = (\phi, m) = \int_0^{\phi} (1 - m \sin^2 \theta)^{1/2} d\theta \tag{A5}$$

$$E_2 = (\phi, m) = \int_0^{\phi} (1 - m \sin^2 \theta)^{-1/2} d\theta \tag{A6}$$

The integration I_2 in Eq. (11) is

$$I_2 = \int_0^{2\pi} \frac{b - y \sin\phi}{(b^2 + z^2 - 2yb \sin\phi)^{3/2}} d\phi = \frac{1}{bnp^2} \left\{ s \left[E_1\left(\frac{\pi}{4}, \frac{-4yb}{n^2}\right) + E_1\left(\frac{3\pi}{4}, \frac{-4yb}{n^2}\right) \right] + p^2 \left[E_2\left(\frac{\pi}{4}, \frac{-4yb}{n^2}\right) + E_2\left(\frac{3\pi}{4}, \frac{-4yb}{n^2}\right) \right] \right\} \tag{A7}$$

where

$$m^2 = b^2 + y^2 + z^2 \tag{A8}$$

$$n^2 = (b-y)^2 + z^2 \tag{A9}$$

$$p = (b+y)^2 + z^2 \tag{A10}$$

$$s = b^2 - y^2 - z^2 \tag{A11}$$

The elliptic integrals of Eq. (A7) are

$$E_1 = (\phi, m) = \int_0^{\phi} (1 - m \sin^2 \theta)^{1/2} d\theta \tag{A12}$$

$$E_2 = (\phi, m) = \int_0^{\phi} (1 - m \sin^2 \theta)^{-1/2} d\theta \tag{A13}$$

References

[1] Wiederick, H. H., Gauthier, N., Campbell, D. A., and Rochon, P., 1987, "Magnetic Braking: Simple Theory and Experiment," Am. J. Phys., **55**(6), pp. 500–503.

[2] Heald, M. A., 1988, "Magnetic Braking: Improved Theory," Am. J. Phys., **56**(6), pp. 521–522.

[3] Cadwell, L. H., 1996, "Magnetic Damping: Analysis of an Eddy Current Brake Using an Airtrack," Am. J. Phys., **64**, pp. 917–923.

[4] Lee, K. J., and Park, K. J., 1998, "A Contactless Eddy Current Brake System," IEEE Conf. on Intelligent Processing Systems, Gold Coast, Queensland Australia, Australia, December, pp. 193–197.

[5] Genta, G., Delprete, C., Tonoli, A., Rava, E., and Mazzocchetti, L., 1992, "Analytical and Experimental Investigation of a Magnetic Radial Passive Damper," in Proceedings of the Third International Symposium on Magnetic Bearings, July, Washington D.C., pp. 255–264.

[6] Kligerman, Y., Grushkevich, A., Darlow, M. S., and Zuckerberger, A., 1995, "Analysis and Experimental Evaluation of Inherent Instability in Electromagnetic Eddy-Current Dampers Intended for Reducing Lateral Vibration of Rotating Machinery," in Proceedings of ASME, 15th Biennial Conference on Vibration and Noise, Boston, MA, pp. 1301–1309.

[7] Karnopp, M., 1989, "Permanent Magnet Linear Motors Used as Variable Mechanical Damper for Vehicle Suspensions," Veh. Syst. Dyn., **18**, pp. 187–200.

[8] Schmid, M., and Varga, P., 1992, "Analysis of Vibration-Isolating Systems for Scanning Tunneling Microscopes," Ultramicroscopy, **42–44**, Part B, pp. 1610–1615.

[9] Teshima, H., Tanaka, M., Miyamoto, K., Nohguchi, K., and Hinata, K., 1997, "Effect of Eddy Current Dampers on the Vibrational Properties in Superconducting Levitation Using Melt-processed YbaCuO Bulk Superconductors," Physica C, **274**, pp. 17–23.

[10] Lee, J. S., 1996, "Dynamic Stability of Beam Plates in Transverse Magnetic Fields," J. Eng. Mech., **122**(2), pp. 89–94.

[11] Kobayashi, H., and Aida, S., 1993, "Development of a Houde Damper Using Magnetic Damping," Vib. Isol., Acoust. Damp. Mech. Syst. ASME, **62**, pp. 25–29.

[12] Kienholtz, D. A., Pendleton, S. C., Richards, K. E., and Morgenthaler, D. R., 1994, "Demonstration of Solar Array Vibration Suppression," Proceedings of SPIE's Conference on Smart Structures and Materials, Orlando, FL, Feb. 14–16, Vol. 2193, pp. 59–72.

[13] Hahn, K. D., Johnson, E. M., Brokken, A., and Baldwin, S., 1998, "Eddy Current Damping of a Magnet Moving Through a Pipe," Am. J. Phys., **66**(12), pp. 1066–1076.

[14] Graves, K. E., Toncich, D., and Iovenitti, P. G., 2000, "Theoretical Comparison of Motional and Transformer EMF Device Damping Efficiency," J. Sound Vib., **233**(3), pp. 441–453.

[15] Morisue, T., 1990, "Analysis of a Coupled Problem: The Felix Cantilevered Beam," IEEE Trans. Magn., **26**(2), pp. 540–543.

[16] Takagi, T., Tani, J., Matsuda, S., and Kawamura, S., 1992, "Analysis and Experiment of Dynamic Deflection of a Thin Plate With a Coupling Effect," IEEE Trans. Magn., **28**(2), pp. 1259–1262.

[17] Matsuzaki, Y., Ishikubo, Y., Kamita, T., and Ikeda, 1997, "Vibration Control System Using Electromagnetic Forces," J. Intell. Mater. Syst. Struct., **8**, pp. 751–756.

[18] Matsuzaki, T., Ikeda, T., Nae, A., and Sasaki, T., 2000, "Electromagnetic Forces for a New Vibration Control System: Experimental Verification," Smart Mater. Struct., **9**(2), pp. 127–131.

[19] Kwak, M. K., Lee, M. I., and Heo, S., 2003, "Vibration Suppression Using Eddy Current Damper," Korean Soc. Noise Vib. Eng., **13**, pp. 760–766.

[20] Bae, J. S., Kwak, M. K., and Inman, D. J., 2004, "Vibration Suppression of Cantilever Beam Using Eddy Current Damper," J. Sound Vib., **284**, pp. 805–824.

[21] Sodano, H. A., Bae, J. S., Inman, D. J., and Belvin, W. K., 2004, "Concept and Model of Eddy Current Damper for Vibration Suppression of a Beam," J. Sound Vib., **288**(4–5), pp. 1177–1196.

[22] Lee, K., and Park, K., 2002, "Modeling Eddy Currents With Boundary Conditions by Using Coulombs Law and the Method of Images," IEEE Trans. Magn., **38**(2), pp. 1333–1340.

[23] Cheng, D. K., 1992, *Field and Wave Electromagnetics*, Addison-Wesley Publishing Company, Reading, MA.

[24] Allemang, R. J., and Brown, D. L., 1998, "A Unified Matrix Polynomial Approach to Modal Identification," J. Sound Vib., **211**(3), pp. 301–322.